Bioactive Materials 6 (2021) 1827–1838

Contents lists available at ScienceDirect

Bioactive Materials

journal homepage: www.sciencedirect.com/journal/bioactive-materials

Procyanidins-crosslinked small intestine submucosa: A bladder patch promotes smooth muscle regeneration and bladder function restoration in a rabbit model

Xiu-Zhen Zhang [a,1], Yan-Lin Jiang [a,1], Jun-Gen Hu [a], Long-Mei Zhao [a], Qiu-Zhu Chen [a], Yan Liang [b], Yi Zhang [b], Xiong-Xin Lei [a], Rui Wang [a], Yi Lei [a], Qing-Yi Zhang [a], Jesse Li-Ling [a], Hui-Qi Xie [a,*]

[a] Laboratory of Stem Cell and Tissue Engineering, Orthopedic Research Institute, State Key Laboratory of Biotherapy and Cancer Center, West China Hospital, Sichuan University and Collaborative Innovation Center of Biotherapy, Chengdu, Sichuan, China
[b] Research Core Facility of West China Hospital, Sichuan University, Chengdu, Sichuan, China

ARTICLE INFO

Keywords:
Bladder reconstruction
Small intestinal submucosa
Procyanidins
Bio-crosslinking
Smooth muscle regeneration

ABSTRACT

Currently the standard surgical treatment for bladder defects is augmentation cystoplasty with autologous tissues, which has many side effects. Biomaterials such as small intestine submucosa (SIS) can provide an alternative scaffold for the repair as bladder patches. Previous studies have shown that SIS could enhance the capacity and compliance of the bladder, but its application is hindered by issues like limited smooth muscle regeneration and stone formation since the fast degradation and poor mechanical properties of the SIS. Procyanidins (PC), a natural bio-crosslinking agent, has shown anti-calcification, anti-inflammatory and anti-oxidation properties. More importantly, PC and SIS can crosslink through hydrogen bonds, which may endow the material with enhanced mechanical property and stabilized functionalities. In this study, various concentrations of PC-crosslinked SIS (PC-SIS) were prepared to repair the full-thickness bladder defects, with an aim to reduce complications and enhance bladder functions. *In vitro* assays showed that the crosslinking has conferred the biomaterial with superior mechanical property and anti-calcification property, ability to promote smooth muscle cell adhesion and upregulate functional genes expression. Using a rabbit model with bladder defects, we demonstrated that the PC-SIS scaffold can rapidly promote *in situ* tissue regrowth and regeneration, in particular smooth muscle remodeling and improvement of urinary functions. The PC-SIS scaffold has therefore provided a promising material for the reconstruction of a functional bladder.

1. Introduction

The main function of the bladder is to store large amount of urine at low pressure and to enable controlled urination. Under certain conditions such as congenital disorder, bladder exstrophy, innervation defects, inflammation and cancer, the bladder may require reconstructive procedures to enlarge its capacity, reduce pressure, and remove the abnormal tissues [1,2]. Currently, the standard surgical treatment is to augment or replace the diseased bladder with tissues derived from small bowel, large bowel or stomach [3,4]. However, such procedures have several side effects. Firstly, these will result in secondary injury to the donor site. Secondly, due to the incompatibility of gastrointestinal segments with bladder, can lead to a variety of complications, including metabolic disturbance, mucus production, urinary tract infection, stone formation, and even secondary malignancies [1,5].

With the advances of tissue engineering, whole organ engineering and bioprinting techniques, diverse materials of distinct properties have been used as acellular scaffolds or tissue substitutes in bladder repair, including decellularized extracellular matrix (ECM) scaffolds, natural or synthetic polymers, and composite materials [6]. Membrane-shaped small intestinal submucosa (SIS) is a bio-derived ECM material mainly composed of collagen, glycosaminoglycans, glycoprotein and a variety

* Corresponding author. Laboratory of Stem Cell and Tissue Engineering, Orthopedic Research Institute, State Key Laboratory of Biotherapy and Cancer Center, West China Hospital, Sichuan University and Collaborative Innovation Center of Biotherapy, No.1, Keyuan 4th Road, Chengdu, Sichuan, 610041, China.
E-mail address: xiehuiqi@scu.edu.cn (H.-Q. Xie).
[1] These authors contributed equally to this work.

https://doi.org/10.1016/j.bioactmat.2020.11.023
Received 23 July 2020; Received in revised form 11 November 2020; Accepted 13 November 2020

of growth factors [7,8]. For its low immunogenicity and good biocompatibility, SIS has been approved by the FDA for various clinical applications, including stress urinary incontinence, urethral and vaginal fistulae, repair of inguinal and vaginal defect for cystocele and rectoceles, and treatment of enteroceles disease. Knapp et al. made the first attempt to use SIS patch to augment porcine bladder in 1994 [9]. Since then, the feasibility of SIS for bladder regeneration has been explored with a variety of animals including rat, rabbit, dog and pig [10–12]. Such studies have demonstrated improved bladder capacity and compliance, yet problems such as contracture, limited smooth muscle regeneration and stone formation have not been fully addressed owning to the fast degradation and poor mechanical properties of SIS, hindering its prospect as an effective treatment strategy [13–16].

Crosslinking has been generally used as a strategy to improve the mechanical and stability of biomaterials [17–20]. For SIS, crosslinking can significantly improve its performance and expand its applications [21]. Glutaraldehyde (GA) is the most widely used crosslinking agent at present. GA crosslinked bovine pericardium has been used in clinic, but side-effects such as calcification and cytotoxicity have been reported [22], which is undesirable for ECM materials in soft tissue repair. As a crosslinking agent, procyanidin (PC) is a naturally derived polyphenols which has shown functions including anti-calcification, anti-inflammation, anti-oxidation, *etc*. [22–25] Furthermore, its metabolic pathways have been well studied *in vivo* [26], and its safety for clinical application has been proved [27]. Han et al. reported that the phenolic hydroxyl in PC can form hydrogen bonds with amide in collagen, which can enhance stability and improve the mechanical properties of the crosslinked material [27,28]. Previous research also showed PC crosslinking can effectively inhibit calcification of valvular ECM material [29,30].

We hereby hypothesized that the introduction of PC crosslinker can modify the properties of SIS and endow various new functions to it, making it a more suitable bladder patch. In this study, we prepared PC-crosslinked SIS material, evaluated its biological properties *in vitro*, and explored its potential as a bladder patch in a rabbit model for full-thickness bladder defect.

2. Materials and methods

2.1. Preparation and characterization of SIS and PC-SIS

2.1.1. Preparation of SIS and PC-SIS

SIS was prepared as previously described [31]. Fresh pig intestines were cleaned, followed by removal of the muscularis, the mucosa, and the serosa. The residual submucous membranes were then soaked in a chloroform-methanol solution (1:1/V:V). After rinsing thoroughly, decellularization was performed with trypsin and SDS in sequence. After rinsing with water thoroughly, the membranes were lyophilized.

To prepare PC-SIS, SIS was immersed in various concentration of PC (Tianjin Jianfeng, China) solution (0.1 ~ 5 mg/ml) for 24 h at 37 °C with continuous shaking in dark, followed by rinsing with water thoroughly, lyophilization, and sterilization.

2.1.2. Morphological analysis

The surface morphology of SIS and PC-SIS samples were characterized by SEM (JSM-6500LV, Jeol, Japan) operated at 15 kV. The freeze-dried scaffolds were cut into 10 mm × 10 mm small pieces, coated with Au, and observed with a SEM at a magnification of 500X.

2.1.3. Analysis of crosslinking degree

Relative efficiency of the crosslinking reagents was measured by monitoring the amount of free amino groups in SIS with ninhydrin according to Ref. [7,32]. In short, 1.5 mg of PC-SIS or SIS were soaked in 1 ml of ninhydrin solution, then bathed in 100 °C water for 20 min, cooled to room temperature, mixed with 5 ml 50% isopropanol by vortex. The absorbance at 570 nm was measured with a spectrophotometer (SYNERGY H1, BioTek, USA). The content of free amino groups in PC-SIS was calculated based on a glycine standard curve. The crosslinking degree is measured by the following formula: Degree of crosslinking = $(M_1 - M_2)/M_1 \times 100\%$ where "M_1" and "M_2" are the molarity of free NH_2 remaining in SIS and PC-SIS scaffolds, respectively.

2.1.4. Chemical bonds analysis

FTIR (Nicolet 6700, Thermo, USA) was used to assess the formation of chemical bond after the crosslinking. The spectra ranges were set as 4000 to 500 cm^{-1}.

2.1.5. Hydrophilicity assay

The hydrophilicity of the materials was detected by the water contact angle tester (DSA30, Kruss, Germany). Dropped water was added onto the sample surface and the picture was captured (n = 5). Contact angles analysis were performed by the equipped analysis software DSAI.

2.1.6. Mechanical properties

The SIS and PC-SIS were cut into dumbbell shape (40 mm × 10 mm) and the bladder specimens from the defect/repair area were cut into a size of 50 mm × 10 mm (n = 4 for each group) for mechanical properties test. The elastic modulus and load of the samples were tested by a mechanical stretcher (Instron 8874, USA). The tests were executed at a 10 mm/min stretch rate till the samples cracked. The detected maximum load was recorded, and the elastic modulus was calculated by the slope of the stress-strain curve.

2.1.7. Primary culture of rabbit bladder smooth muscle cells (R-B-SMCs)

Primary culture of R-B-SMCs were performed as previously described [33]. Firstly, bladder tissues obtained from New Zealand white rabbit were washed with PBS. Then, the mucosa and serous membrane of the bladder tissues were stripped to expose the smooth muscle. The smooth muscle tissue was treatment with 0.25% trypsin (Gibco, USA) at 37 °C for 20 min, followed by cutting up small pieces, then incubated in 0.1 mg/ml type I collagenase (Sigma, USA) for 20 min. The cell suspension was filtered with a 70 μm mesh. R-B-SMCs were collected and cultured in DMEM (with 10% FBS and 1% penicillin/streptomycin (Gibco, USA)). The R-B-SMCs were determined by immunofluorescent staining, which was performed by incubation with primary antibody (α-SMA (1:500 diluted, ab32575, Abcam), Myosin (1:500 diluted, ab11083, Abcam) and Desmin (1:200 diluted, ab8976, Abcam)), secondary antibody and DAPI in sequence.

2.1.8. Cytotoxicity assay

The cytotoxicity of SIS and PC-SIS was evaluated by CCK-8 (Dojindo, Japan) assay with R-B-SMCs. Briefly, the extract was prepared by soaking the materials in culture medium at 37 °C incubator for 24 h. R-B-SMCs were seeded in 96-well at 1×10^4 cells per-well. After cell attachment, replaced with the prepared extract. Complete medium was used as control. The medium was changed every 2 days. Cell proliferation was tested on day 1, 3, 5 and 7.

Live/dead staining was applied to assess the biocompatibility of the materials. R-B-SMCs was seeded onto the materials and cultured for 5 days, with medium change every other day, then stained with Calcein-AM and PI Double Stain Kit (Dojindo, Japan) for 20 min at 37 °C in the darkness. The samples were then imaged with a confocal microscope (Nikon A1RMP+, Nikon Instruments Inc., Tokyo, Japan).

2.1.9. Enzyme hydrolysis assay

Enzymatic hydrolysis of materials was executed *in vitro* to assess the degradation properties as previously described [22]. Briefly, the samples were cut into small discs (diameter = 15 mm) and sterilized prior to the testing. Samples were then immersed in a collagenase-II solution and maintained at 37 °C for various periods of time (1, 2, 4, 24 h) with continuous shaking. The enzymatic hydrolysis rate was calculated as described by Wang et al. [7].

2.1.10. Dynamic release of PC from PC-SIS

The release of PC from PC-SIS was measured as previously described [15]. Firstly, the PC-SIS was soaked in D-Hanks solution allowing for PC release. Then, the sample solution was reacted with vanillin/HCl solution (1:2/V:V) for 25 min. Then the absorbance at 500 nm was detected by spectrophotometry. The standard curve was determined with PC solutions of known concentrations.

2.1.11. Anti-calcification assay

The anti-calcification property of the scaffolds was determined in simulated body fluid (SBF) as previously described [34]. SIS and PC-SIS were immersed in SBF (10 ml/cm^2) at 37 °C for 14 days, followed by washing and drying. Then the samples were characterized under a SEM and energy-dispersive spectrometer (SEM/EDS, INCA Energy, Oxford Instruments, UK). To quantify the concentrations of Ca/P elements on the scaffolds, the remaining sample was dissolved in 0.2 M HCl, and the Ca/P contents were detected with inductively coupled plasma atomic emission spectroscopy (ICP-AES; VISTA AX, Varian). The mineralization was also determined by Alizarin red staining [35].

2.1.12. Animal experiments

All animal experiments were approved by Sichuan University Animal Care and Use Committee (No.2018190A) in accordance with the Principles of Laboratory Animal Care formulated by the National Society for Medical Research.

2.1.13. Histocompatibility

The histocompatibility and degradation of the material *in vivo* were assessed by subcutaneous implantation. A total of 12 male SD rats (200–220 g) was divided into 6 groups according to the PC concentration. Two skin incisions were made on the back, then the SIS and PC-SIS scaffolds (10 mm × 10 mm) were implanted subcutaneously. After 3 weeks, the implants and near tissues were collected for histological evaluation.

2.1.14. Bladder repair

Forty-eight male New Zealand white rabbits (2.5 ± 0.5 kg) was divided into four groups (Sham, SIS, PC-SIS 1 and PC-SIS 2). Briefly, the rabbits were anesthetized through injection of pentobarbital sodium (2 ml/kg) through the marginal vein. A paramedian incision was made at the lower abdomen to expose the bladder. Part of full thickness bladder wall (circa 2 cm × 2 cm) was excised to construct a model for a defect on the posterior wall. Sterilized SIS, PC-SIS 1 or PC-SIS 2 (circa 2.2 cm × 2.2 cm) was sewn into place with degradable sutures (5-0 Monocryl, Johnson & Johnson, USA). Non-resolvable sutures (5-0 Monocryl) were made to mark the square defect in the serosa layer. The abdomen was then closed by suturing the muscle and skin (Video S1 and Fig. S1). Penicillin (400,000 units/day, Harbin Pharmaceutical Group Holding Co.) was given through intramuscular injection daily for 3 days. At the sampling time points (4, 8 and 12 weeks), the rabbits were euthanized, and the hypogastrium was opened for observing the adhesion in the surgical area. The fat pad was then dissected from the bladder, and the inner wall of the bladder was subjected to macroscopic examination for calculus formation, material degradation and scarring. The bladder tissues and the kidneys were then collected for histology analysis. In addition, blood samples were collected for hematology analysis, including blood cell counts, serum electrolytes, hepatic and renal function indicators.

Supplementary data related to this article can be found at https://doi.org/10.1016/j.bioactmat.2020.11.023.

Histology

Tissue samples were rinsed with 0.9% NaCl, then fixed with 10% formalin, gradient alcohols was dehydrated and paraffin-embedded, sectioned at 3–5 μm for H&E staining. Immunofluorescence staining was also performed with various primary antibodies including AE1/AE3 (1:500 diluted, ab9377, Abcam), Uroplakin III (1:100 diluted, ab78196, Abcam), α-SMA (1:200 diluted, ab32575, Abcam), Myosin (1:500 diluted, ab11083, Abcam), SYP38 (1:100 diluted, ab8049, Abcam), and CD31 (1:100 diluted, ab199012, Abcam), followed by incubation of the secondary antibodies as well as DAPI. Image Pro Plus was applied to analyze the images, including the percentage of positive staining area, and the number of vessels.

Ultrasonography and analysis of stone composition

The bladder was examined by ultrasound at various time points. Pre-warmed sterile saline was injected into the bladder via an 8 F catheter until maximum distension. Ultrasonography was carried out on a PHILIPS IU22 ultrasound system (Philips, Best, Netherlands). Bladder stone samples were collected, grinded by quartz dish, and further analyzed by a second-generation stone analysis machine (Lanmode LIR-20).

Urodynamics

Bladder function was determined by urodynamics without anesthesia at 12 weeks post operation. Urodynamics were determined with a urodynamic system (Nidoc 970A+, Chengdu, China) as described elsewhere [36]. The urodynamic catheter was inserted into the rectum and urethra, respectively, and connected with the urodynamic system. Pre-warmed normal saline was injected into the bladder at a rate of 20 ml/min, while the volume of saline, the intravesical pressure (P_{ves}), and the abdominal pressure (P_{abd}) were simultaneously monitored. When the first fluid leakage was noted, the intravesical pressure and bladder capacity were measured, and the bladder compliance was calculated by the difference value of the P_{ves} and the P_{abd}.

Effects of PC crosslinking on R-B-SMCs

Cell adhesion

Cell adhesion was assessed by cytoskeletal staining and SEM. Initially, R-B-SMCs were respectively seeded on the materials at 1×10^4 cells per-well in 24-well plates and cultured for 5 days.

For cytoskeletal staining, the cell-scaffolds constructs were washed by PBS, then fixed with 4% paraformaldehyde. Thereafter, the constructs were treated in 0.1% TritonX-100, and incubated with rhodamine-phalloidin (Solarbio, Shanghai, China) and DAPI. After washing thoroughly, the constructs were visualized by confocal laser microscopy (Nikon A1RMP+, Nikon Instruments Inc., Tokyo, Japan).

For SEM detection, the constructs were fixed with 2.5% glutaraldehyde and critical-point dried with CO_2. The cell morphology were observed by SEM (JSM-6500LV, Jeol, Japan).

Quantitative real-time PCR

Total RNA was extracted from cultured cell-scaffold complex using Trizol reagent following the manufacturer's protocol, followed by reverse transcription (RR047, Takara, Japan). Quantitative PCR was performed using SYBR Green master mix (RR820, Takara, Japan) on a real-time thermocycler (LC 96, Roche, Switzerland). The thermal cycle program was as follows: 95 °C for 30 s; 40 cycles of 95 °C for 10 s and 60 °C for 30 s. The PCR primers were listed in Table S1. The relative expression folds were calculated by the $2^{-\triangle\triangle Ct}$ method.

Statistical analysis

All values are presented as mean ± SD. Statistical analysis was carried out using the Student's t-test or one-way ANOVA with Tukey's test *post hoc*. $P < 0.05$ was considered to be statistically significant.

3. Results

Preparation and basic characterization of PC-SIS

SIS was initially crosslinked with PC of different concentrations (0.1–5 mg/ml). As shown in Fig. 1A, the PC-SIS scaffolds were soft,

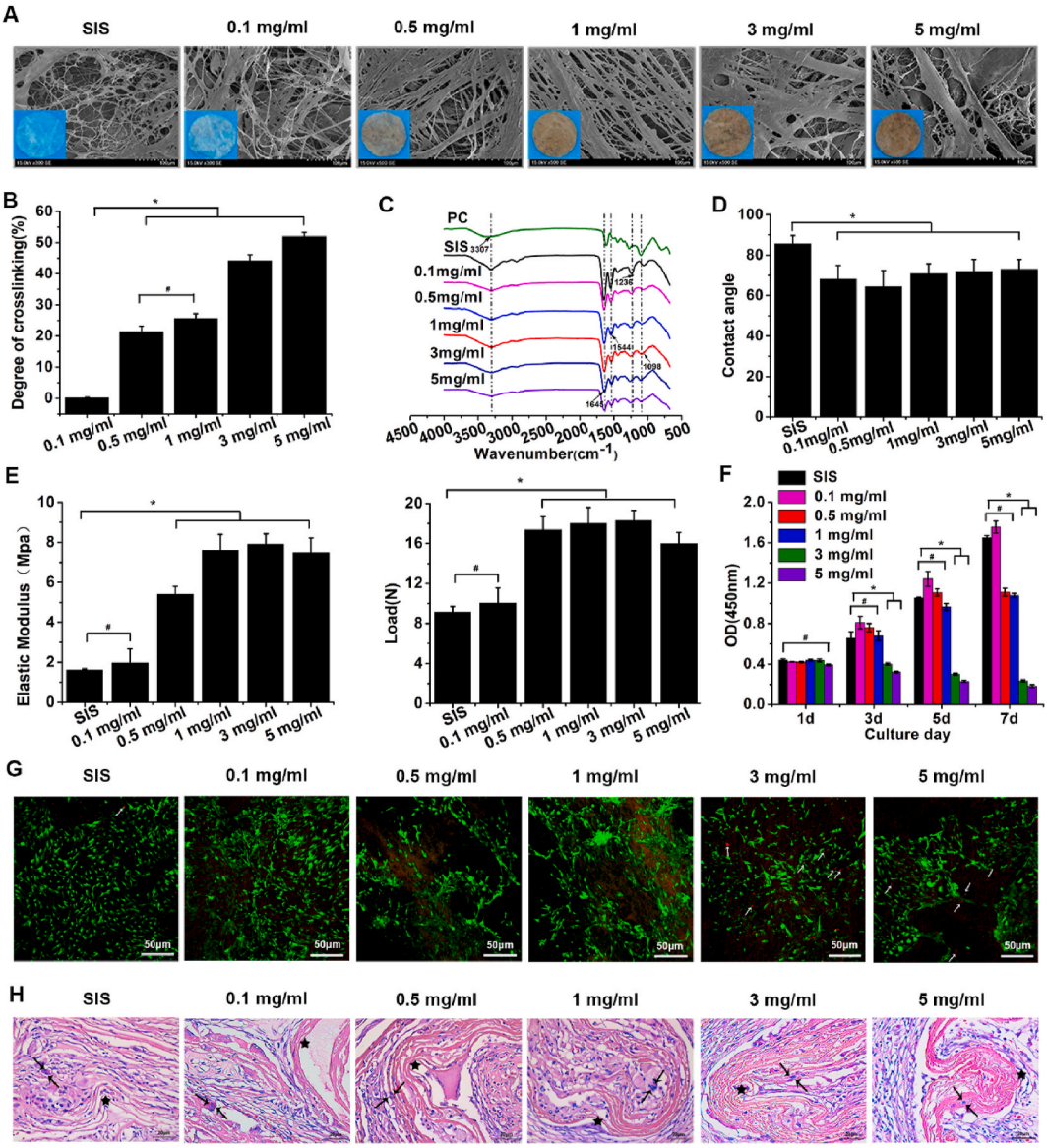

Fig. 1. Optimal crosslinking concentration of PC *in vitro*. (A) Gross observation and ultrastructure of the material under a scanning electron microscope (SEM) of all groups. Scale bars = 100 μm. (B) Degree of crosslinking of PC-SIS as calculated based on the Ninhydrin assay. *$P < 0.05$. #$P > 0.05$. (C) Fourier transforms infrared spectral (FTIR) analysis. (D) Measurement of water contact angle of the materials with different concentration of crosslinker. *$P < 0.05$. (E) Characterization of the mechanical properties of various materials. *$P < 0.05$. #$P > 0.05$. (F) Cell proliferation in various groups as detected with a CCK-8 assay. Data was presented as mean ± S.D. *$P < 0.05$. #$P > 0.05$. (G) Viability of the cell on various materials as assessed by Calcein AM/PI staining. Scale bars = 50 μm. (H) Subcutaneous implantation of representative scaffolds 3 weeks postoperatively. ★Indicates scaffolds, →Indicates inflammatory cells. Scale bar = 50 μm.

stretchable, and did not shrink. As the PC concentration increased, the PC-SIS gained a deeper palm red color. SEM results indicated that the SIS had a porous surface consisted of collagen fibers, while the fibers of PC-SIS had a greater diameter with better directional arrangement. The degree of crosslinking was determined by quantifying the free amino group, which ranged from 0.2% to 65% as PC ranged 0.1–5 mg/ml (Fig. 1B). Particularly, PC with a concentration higher than 0.5 mg/ml could effectively crosslink SIS (Fig. 1B). Indeed, as illustrated by ATR-FTIR (Fig. 1C), the hydrogen bond absorption peaks (3307 cm^{-1}) of PC-SIS became wider as the concentration of PC increased, indicating more hydrogen bonds i.e. higher crosslinking degree. PC crosslinking also resulted in lower contact angle (Fig. 1D), indicating higher hydrophilicity. As discovered, the collagen content could drop to 67.25 ± 7.04° (0.5 mg/ml PC-SIS group) and 48.75 ± 8.27° (1 mg/ml PC-SIS group) compared with the SIS group (85.25 ± 6.11°).

The mechanical properties and the cyto-/his-compatibility of PC-SIS were further characterized. The max load and elastic modulus increased significantly when PC reached 0.5 mg/ml, but plateaued when PC reached 1 mg/ml (Fig. 1E). The cytocompatibility of PC-SIS was assessed with rabbit bladder smooth muscle cells (R-B-SMCs) by a CCK-8 assay and a live/dead staining assay, and the histocompatibility of PC-SIS was assessed by subcutaneous implantation in rat. As shown in Fig. 1F, SIS and 0.1 mg/ml PC-SIS could support the proliferation of R-B-SMCs, while 0.5 and 1 mg/ml PC-SIS showed mild cytotoxicity (less R-B-SMCs proliferation). When PC 3 mg/ml, the proliferation of R-B-SMCs was suppressed. By live/dead staining (Fig. 1G), obvious dead cells were also observed when PC reached 3 mg/ml. Subcutaneous implantation of PC-SIS did not induce significant inflammatory responses in all concentration groups (Fig. 1H). According to above results, 0.5 mg/ml (PC-SIS 1) and 1 mg/ml PC-SIS (PC-SIS 2) showed improved mechanical properties, acceptable cytocompatibility, and good histocompatibility. Hence, such two PC-SIS materials were selected for subsequent experiments.

Characterization of the potential physiological functions of PC-SIS in vitro

The *in vitro* enzymatic degradations of PC-SIS 1 and PC-SIS 2 were characterized. As shown in Fig. 2A, PC crosslinking can generally decrease the enzymatic degradation rate, which may contribute to better application potential of PC-SIS as a bladder patch. In addition, considering that PC has anti-inflammatory and anti-oxidative activities and that PC crosslinking formed weak hydrogen bonds, the release of PC from the PC-SIS materials was characterized. As shown in Fig. 2B, detectable PC release was noted. Specially, PC-SIS 2 showed a burst release on day 1 (approximately 0.14 ng/mg), followed by a gradual release (approximately 0.06 ng/mg per day) during the testing period. By contrast, the amount of PC released from the PC-SIS 1 was relatively stable from day 1 to day 9 ($P > 0.05$).

Previous studies have shown that PC crosslinked ECM has an anti-calcification effect, so the anti-calcification ability of PC-SIS was evaluated *in vitro* [23]. Alizarin red staining showed that PC-SIS markedly reduced the formation of mineralization nodules (Fig. 2C). SEM-EDS results also revealed the less mineralization deposition on PC-SIS (Fig. 2D). After dissolving the mineralization deposition in acidic solution, the Ca and P were quantified by ICP analysis. As shown in Fig. 2E, PC-SIS had significantly less Ca and P deposition. These results indicated that PC-SIS had anti-calcification activities *in vitro*.

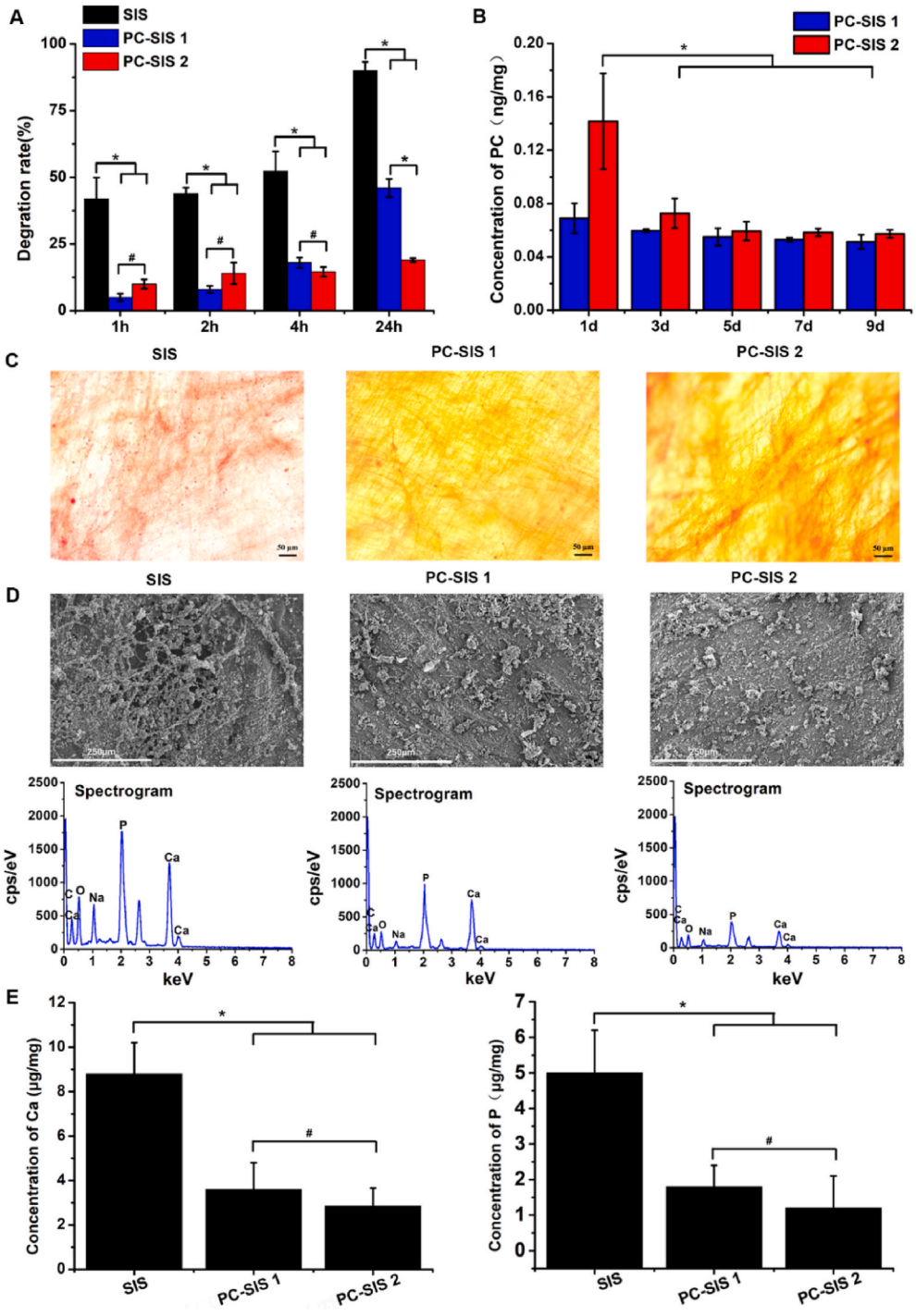

Fig. 2. Properties of the PC-SIS with potential physiological functions. (A) Stability of the material as determined by enzymatic hydrolysis *in vitro*. $*P < 0.05$. $\#P > 0.05$. (B) Sustained release from the crosslinked scaffolds *in vivo* over nine days. $*P < 0.05$. (C) Anti-calcification as determined by Alizarin red S staining. Scale bars = 50 μm. (D) SEM/EDS was used to detect the anti-Calcification effect with various materials. Scale bars = 250 μm. (E) Calcium and phosphorus content were determined by ICP-AES. Data was presented as mean ± S.D. $*P < 0.05$; $\#P > 0.05$. (For interpretation of the references to color in this figure legend, the reader is referred to the Web version of this article.)

Effect of PC crosslinking on R-B-SMCs behaviors

The smooth muscle cells contribute to the contractile functions as well as the compliance of the bladder, whether the PC-SIS material is suitable for bladder repair largely depends on its effects on the bladder SMCs. By *in vitro* assessments, the effects of PC-SIS on SMCs were preliminarily investigated. As shown in Fig. 3A, the cytoskeleton staining showed that in the PC-SIS groups the R-B-SMCs formed a more organized bundle-like structure, while in the SIS group the R-B-SMCs were less organized. By SEM at single cell level (Fig. 3B), the PC-SIS groups especially the PC-SIS 2 group showed that the R-B-SMCs formed filopodia-like connections emerging from the cell body, creating connections with adjacent cells. The PC-SIS groups had a large amount of extracellular matrix deposition, suggesting that the PC-SIS materials were more conducive to cell growth and spreading. As shown in Fig. 3C, the expression of smooth muscle cell-specific genes (α-SMA, Myosin and Desmin) was higher in the PC-SIS groups especially in the PC-SIS 2 group. Taken together, the PC-SIS material could facilitate the organization of smooth muscle cells, enhance the deposition of extracellular matrix, and promote the expression of functional genes.

PC-SIS as a bladder patch in the rabbit defect model

The PC-SIS was then used to repair full-thickness bladder defect to evaluate its potential as a bladder patch. The experimental animals were divided into four groups: the Sham group (no defects in bladder), the SIS group (repaired by SIS), the PC-SIS 1 group (repaired by 0.5 mg/ml PC-SIS), and the PC-SIS 2 group (repaired by 1 mg/ml PC-SIS). Bladder

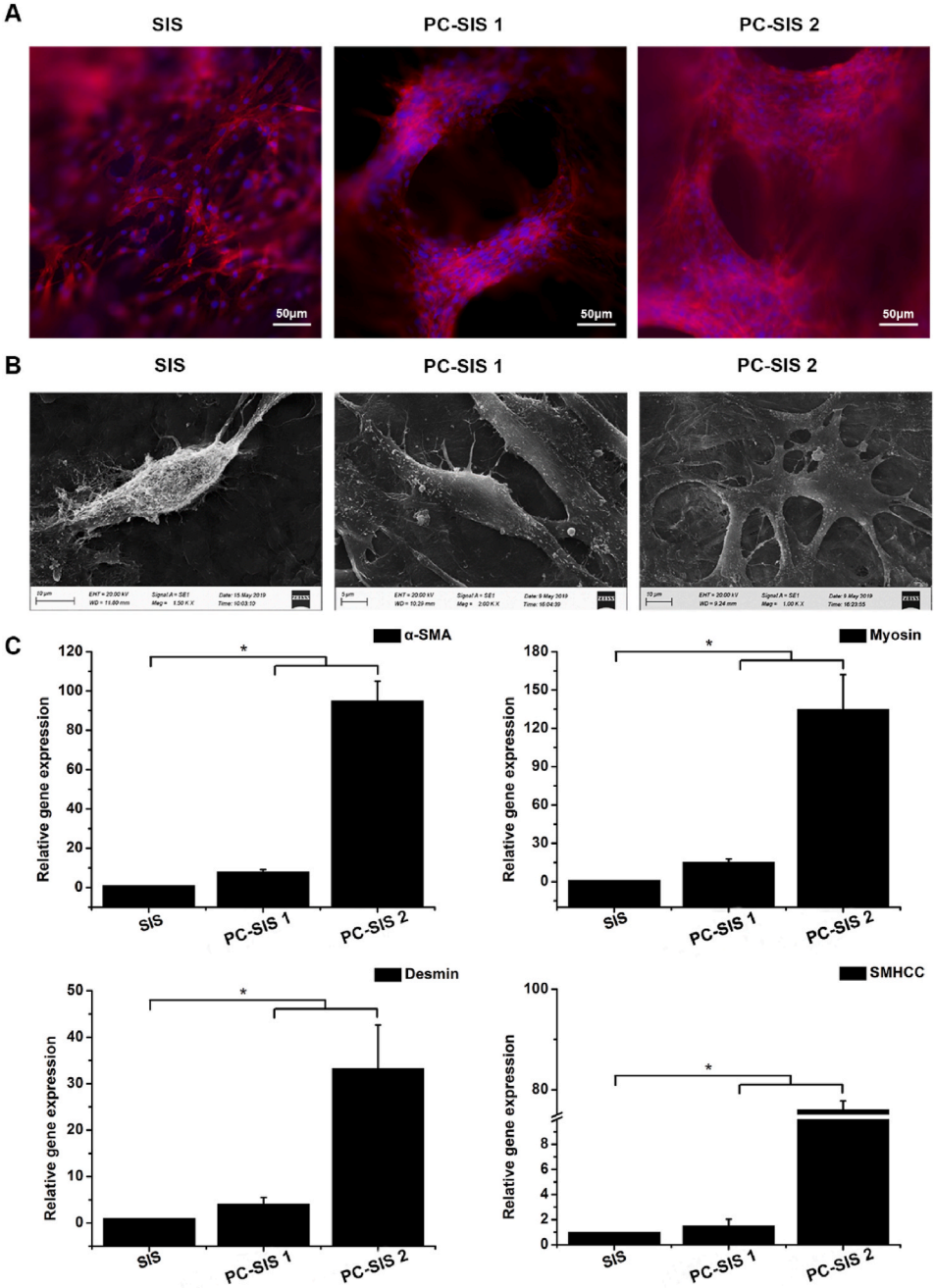

Fig. 3. Effect of crosslinking on R-B-SMCs. (A) F-actin staining showed the cytoskeleton on the different materials after 5 days culture. Scale bars = 50 μm. (B) SEM indicated the ultrastructure of R-B-SMCs on the different crosslinker materials after 5days culture. Scale bars = 5 μm & 10 μm. (C) Quantitative Real-Time PCR detected the smooth muscle-related gene expression on the different materials after 5 days culture. *$P < 0.05$.

tissue of restoration area were collected at scheduled points (4W, 8W& 12W after operation).

When sampling, the bladder tissues were generally observed. Slight adhesion of the sutured area of the bladder with surrounding tissues was noted at all time points (not shown). All experimental groups showed varying contracture of the bladder at 4 weeks, yet the contracture rate has decreased with the elapse of time (Fig. S3). As shown in Fig. S3, negligible scar formation and graft shrinkage were observed at the regeneration sites in the PC-SIS 1 and PC-SIS 2 groups at 12 weeks postoperatively. On the contrary, notable shrinkage was observed in the SIS group. Bladder stones were found only at 4 weeks in the SIS, PC-SIS 1 and PC-SIS 2 groups with an approximately rate of 50%, 50%, and 75%, respectively, with visible biomatrix at the center of the stones. A gross view of kidneys showed no significant signs of hydronephrosis in all groups at 12 weeks postoperatively. H&E staining also indicated normal kidney tissue structure in all groups: no pathological changes or interstitial edema of the glomerular and collecting ducts (Fig. S4). By testing the blood samples of the experimental rabbits, no obvious difference in all four groups (Table S2). It may therefore be concluded that the PC-SIS has no hepatoxicity and nephrotoxicity.

The bladder repair effects of PC-SIS were further evaluated by histology analysis. Revealed by H&E staining, connective tissues had grown into the defect areas from the periphery native tissues in all groups at 4 weeks, yet no obvious smooth muscles were observed at the defect areas (Fig. S5). Interestingly, island-like structures were also found at the basal region of urothelium (Fig. S5), which were putatively related to epithelium regeneration. At 8 weeks, the regenerated epithelium at the defect areas had become multilayered in all groups (Fig. S6), resembling the native bladder urothelium. Meanwhile, some disordered smooth muscle-like tissues and more fibrous tissues were found at the defect areas in the SIS group at 8 weeks (Fig. S6). However, the PC-SIS groups showed a normal tissue organization consisted of longitudinal and/or circular muscle bands, particularly the PC-SIS 2 group (Fig. S5). At 12 weeks, small scattered smooth muscle fibers were found throughout the defect area in the SIS group, while distinct bundles of smooth muscle were evident in the PC-SIS groups (Fig. 4) resembling the native bladder smooth muscles.

The bladder tissues collected at 12 weeks were also evaluated by IF staining: AE1/AE3 and Uroplakin-III for urothelium, α-SMA and Myosin for smooth muscle, SYP38 for nerve fiber, and CD31 for vessels. In consistent with H&E staining results, the IF staining showed that the PC-SIS groups had a more similar urothelium morphology with the Sham group, while SIS group had a thicker urothelium (Fig. 5A and B, $P < 0.05$). Uroplakin-III showed a thinner superficial staining area, demonstrating the different layers of the uroepithelium. No significant differences were observed between the groups. Muscle staining confirmed that, compared with the 0.5 mg/ml PC-SIS group, the 1 mg/ml PC-SIS group had more regularly arranged smooth muscle bundles (Fig. 5C). Regenerated muscle fibers were also found in the SIS group, albeit that the newly formed muscle fibers were much smaller in size and more "naive-like", which suggested incomplete regeneration (Fig. 5C). Quantitative morphometric analysis confirmed that PC-SIS groups had more smooth muscle than the SIS group (Fig. 5D, $P < 0.05$). Positive staining for SYP38 suggested pathological remodeling of normal synaptic transmission areas (Fig. 5E). Compared with the SIS group and the PC-SIS 1 group, PC-SIS 2 group had an increased SYP38-positive area, though significantly smaller than the Sham group (Fig. 5E and F, $P < 0.05$). Similarly, the number of newly formed capillaries in the PC-SIS 2 group were significantly greater than those of the SIS and the PC-SIS 1 groups, demonstrating that the PC-SIS 2 group had better neovascularization (Fig. 5G and H).

In addition to histological analysis, the repair effects were also evaluated by ultrasonic imaging and urodynamics. In consistent with the general observation when sampling, bladder stones were found in all experimental groups at 4 weeks by ultrasonic imaging (Fig. S7A). No stones were found at 8 weeks or 12 weeks (Figs. S7A and 6A). Principal component analysis (PCA) of the bladder stones revealed that the main components were calcium oxalate monohydrate and calcium oxalate dihydrate (Fig. S7B).

Before sampling at 12 weeks, the urodynamics were recorded (Fig. 6B). The SIS group had the lowest P_{det} than the other groups, indicating poor bladder remodeling in consistent with histological results. Bladder compliance, defined as the ratio between changes in bladder volume and detrusor pressure ($P_{det} = P_{ves} - P_{abd}$), was used as an indicator for bladder remodeling and function. As shown in Fig. 6C, the PC-SIS 2 group has a bladder compliance similar to the sham group,

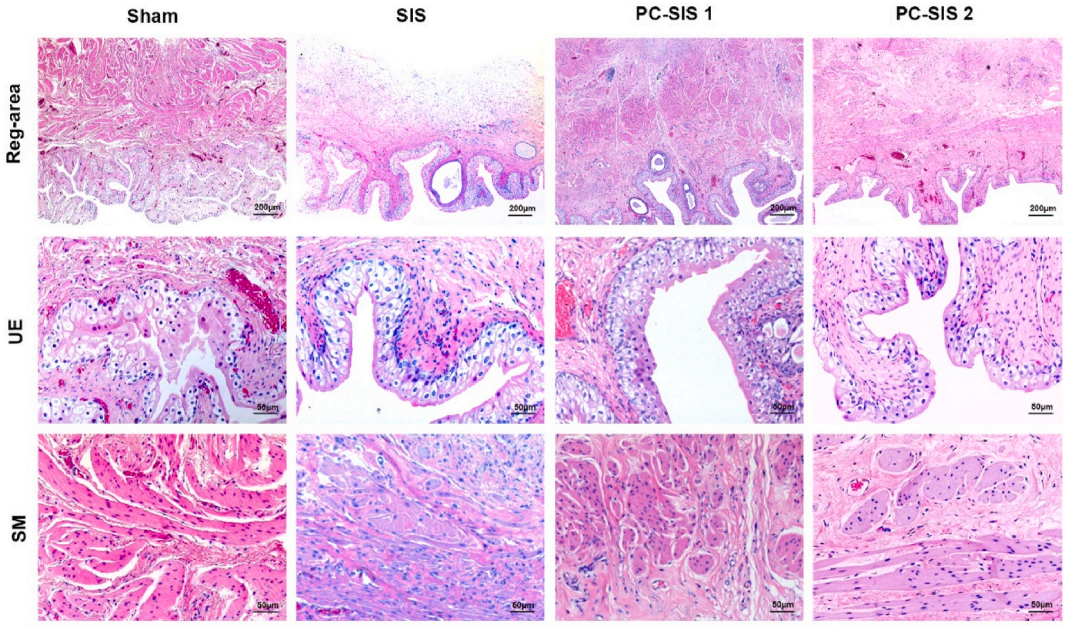

Fig. 4. Histological and morphological evaluation of the regenerated bladder domes in the sham and experimental groups. 1st row: H&E staining indicated the central zone areas in the sham and regenerated bladders. Scale bars = 200 μm. 2nd and 3rd rows: Local expansion of the urothelium (UE) and smooth muscle (SM) bundles displayed in the 1st row. Scale bars = 50 μm.

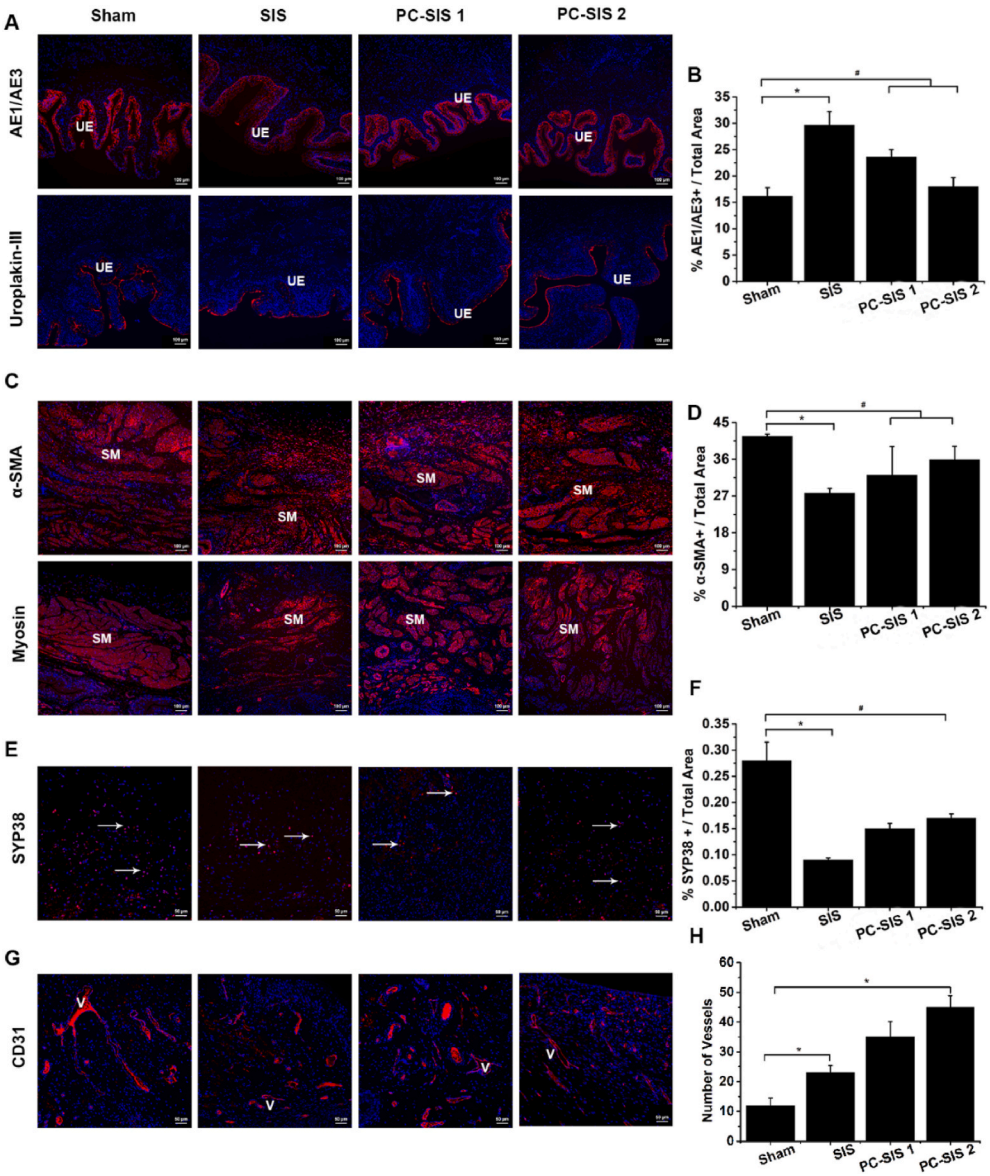

Fig. 5. Immunofluorescence staining and quantitative assessments of the repaired bladder domes in the sham and experimental groups at 12 W after the surgery. (A) Expression of urothelial-associated markers AE1/AE3 and Uroplakin-III. UE, urothelium. Scale bars = 100 μm. (C) Expression of smooth muscle-specific markers α-SMA and Myosin. SM, smooth muscle. Scale bars = 100 μm. (E) The innervation marker, synaptophysin (SYP38). Arrows represented $SYP38^{+}$. Scale bars = 50 μm. (G) The endothelial maker CD31. V denotes $CD31^{+}$ vessels. Scale bars = 50 μm. Specific marker expression was indicated by red (Cy5 labeling) and DAPI staining (blue) marks the nucleus. (B, D & F) Percentage of positive area relative to total area are compared among the three groups. (B) AE1/AE3, (D) α-SMA, (F) SYP38 and (H) Number of CD31-positive vessels. Data was presented as the mean ± S.D. $*P < 0.05$; $\#P > 0.05$. (For interpretation of the references to color in this figure legend, the reader is referred to the Web version of this article.)

as well as the peak intravesical pressure and the bladder capability ($P > 0.05$). After sampling, the mechanical properties of the sample tissues were also tested. The PC-SIS groups showed similar elastic modulus and maximum load with the sham group, while the SIS group had the lowest elastic modulus and maximum load (Fig. 6D).

4. Discussion

Both biological and synthetic degradable biomaterials have been tested for bladder regeneration with various outcomes [37–39]. Conventional tissue engineered bladder patches for augmentation cystoplasty included autologous cell-seeded materials and cell-free scaffold materials. Disadvantages of the seeded strategy included prolonged preparation period, greater cost and risk of exogenous contamination, which hindered its clinical application [40,41]. By contrast, the cell-free strategy is conducive for clinical applications on a large scale, as approved patch products can be off-the-shelf, while native cells recruited by the patch can regenerate tissues *in vivo*. The decellularized SIS material, harvested from the submucosa layer of porcine small intestine, has shown to promote regeneration of various host tissues including the urinary bladder through a series of animal models [42,43].

To overcome the accompanying problems of using SIS in bladder repair, such as contracture, limited smooth muscle regeneration and stone formation, PC appeared to be a good candidate crosslinking agent for modification. Known as a condensed tannin, PC consist of oligomer or polymers of (epi) catechin, whose phenolic hydroxyl structures have the capacity to form intermolecular hydrogen bonds. Unlike epigallocatechin gallate (EGCG), a catechin monomer with pro-osteogenesis activity [44], PC has anti-calcification activity which is favorable for bladder repair. In this study, PC was tested as a crosslinking agent for SIS membrane to generate a cell-free scaffold for their potential for bladder reconstruction.

The crosslinking reaction between PC and SIS involves primarily hydrogen bonding with the amide carbonyl and phenolic hydroxyl of the proteins [45]. SIS is mainly consisted of proline-rich collagen, thus can be crosslinked with PC through formation of strong hydrogen bonds. Furthermore, the helix conformation in the SIS collagen structure could increase the accessibility of hydrogen bond [27]. As shown by ATR-FTIR, the hydrogen bond absorption peaks (3307 cm^{-1}) of PC-SIS became wider compared with that of SIS, which indirectly suggested formation of hydrogen bonds. As shown by SEM results, with the increase in PC concentration, the average diameter of PC-SIS fibers

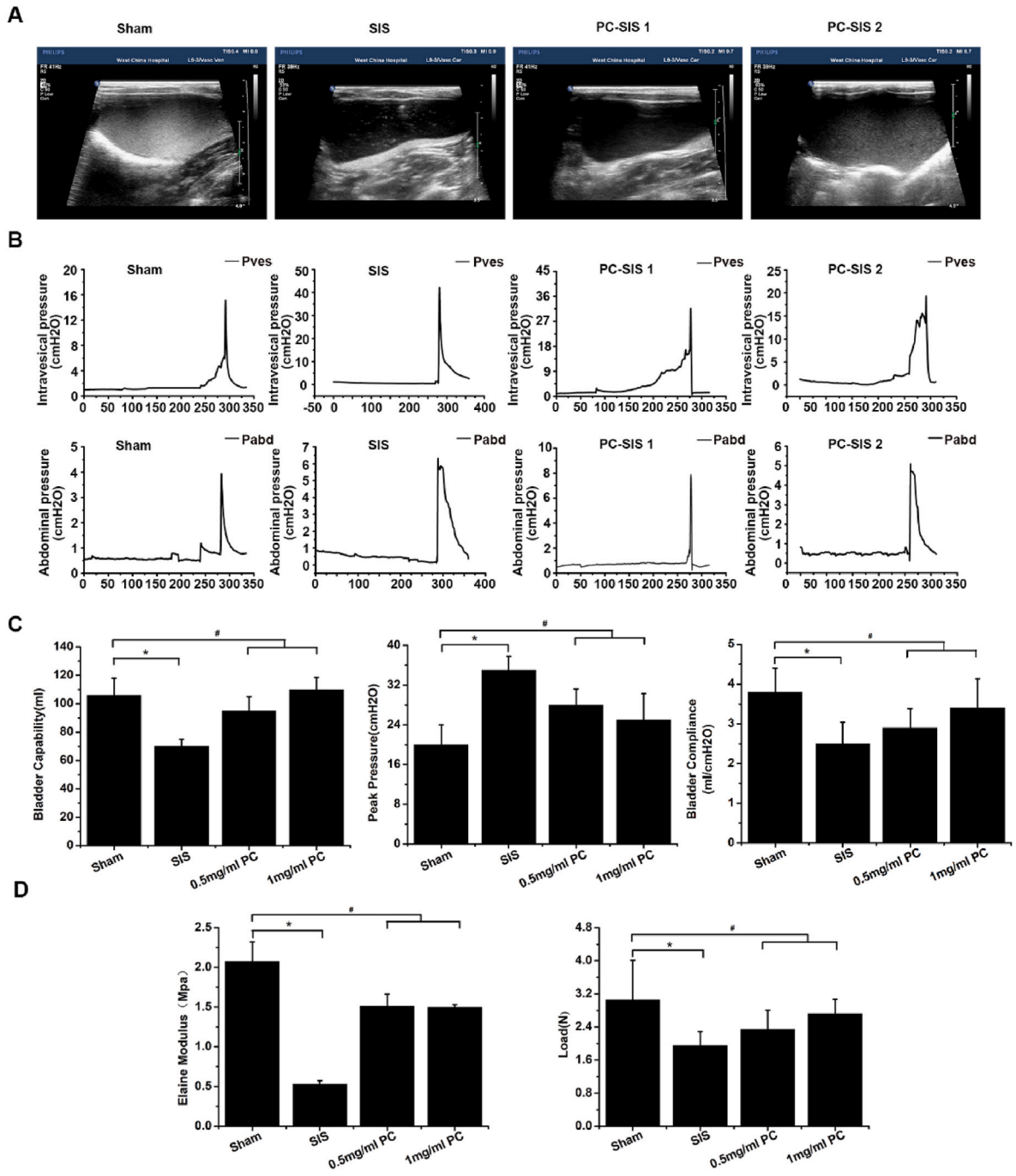

Fig. 6. Evaluation of bladder function through ultrasonic testing (UT) and urodynamic survey (UDS). (A) US Transverse (short axis) ultrasound image of urinary bladder among different groups at 12 W after the surgery. (B) P_{ves}: intravesical pressure; P_{abd}: abdominal pressure. (C) Capacity, peak pressure and compliance of the bladder at 12 W after the surgery. Data was presented as the mean ± S.D. $^*P < 0.05$; $\#P > 0.05$. (D) Characterization of the mechanical properties of various bladder tissues at 12W. $^*P < 0.05$. $\#P > 0.05$.

increased, and the arrangement of the fibers exhibited directionality possibly as the formation of hydrogen bonds. Meanwhile, the large amount of phenolic hydroxyl in the PC molecule also resulted in improved hydrophilicity of the PC-SIS and promotion the attachment of cells.

However, high concentration of PC can also induce toxicity. With the aim to develop a bladder patch, the PC concentration to prepare PC-SIS material was optimized. Based on the mechanical properties and the cyto-/his-compatibility results, 0.5 mg/ml and 1 mg/ml of PC (PC-SIS 1 and PC-SIS 2, respectively) were chosen for subsequent experiments. The degradation of biomaterials is a key issue to be considered. The results showed that crosslinking could enhance the stability of the materials *in vitro*, but whether such degradation rate matched bladder repair needed more experimental evidences. Release of PC itself which has anti-inflammatory and anti-oxidative activities is also an important issue. In the present study, PC-SIS 1 showed a stable release, while PC-SIS 2 showed a burst release in the early stages. Yet, whether such released PC affected the tissue remodeling remained to be clarified. Regarding the calcification of materials, since anionic groups on surface of the material can induce Ca^{2+} nucleation by electrostatic forces which may contribute to mineral deposition [46,47], blocking of such groups may reduce the calcification of materials. SIS contains multiple amino

acids capable of attracting Ca^{2+}, such as proline, glycine, and hydroxyproline. After PC crosslinking, the amount of Ca^{2+} deposition was reduced by at least 50%. These results showed that PC crosslinking could inhibited *in vitro* calcification effectively, possibly due to blocking of the mineral nucleation sites.

The bladder wall expands dramatically during normal filling and emptying, which involves contractions of SMCs. Thus, whether the PC-SIS material is suitable for bladder repair largely depends on its effects on the bladder SMCs. *In vitro* experiments were performed to clarify the biological behaviors of R-B-SMCs on PC-SIS materials. As shown in Fig. 3, IF staining of cytoskeleton suggested that cells cultured on the PC-SIS matrices had a higher degree of cellular bundling, while SEM showed that PC-SIS promoted the formation of adhesion-related structures within the cells. At molecular level, the expression of all SMCs markers increased in the PC-SIS groups especially in the PC-SIS 2 group. Such effects may be mainly resulted from the change of mechanical properties after PC crosslinking. It has been suggested that mechanical changes in the microenvironment alone may drive specific cell behaviors, as supported by the instructional roles of ECM mechanics in cellular behavior and tissue development [48,49]. Indeed, some discoveries implied that mechanical forces participate in the maintenance of SMC phenotype. In smooth muscle tissue engineered models, SMCs may show an osteoblast-like phenotype without cyclic mechanical strain [50–52]. In this study, mechanical behavior of the SIS membranes was significantly influenced by crosslinking to a certain degree favorable for maintaining the phenotype and function of SMCs, though other possible mechanisms may also be involved such as enhancement of cellular adhesion.

After testing the crosslinking efficiency and biological properties of the PC-SIS scaffolds *in vitro*, the implants were assessed in a rabbit model to evaluate its capability for enhancing bladder regeneration. Enhancement of mechanical properties not potentially just affect repair outcomes, but also benefit the handling properties of biomaterials during surgical operations, for example the suturing, which is particularly important for its surgical usability [53]. Though *in vitro* results demonstrated that the PC-SIS had some anti-calcification activity, *in vivo* results showed that bladder stones were found in all experimental groups with similar rates at 4 weeks post operation in consistent with previous studies [39,54]. This may be explained by the fact that on one side the crosslinking blocked some calcium salt deposition sites, but on the other side it enhanced the stability of the foreign material leading to stone formation [55,56]. The nucleation reaction due to the adhesion of urate or calcium oxalate crystals within the remaining biomaterial fragment in the bladder could be a critical step for the formation of encrustation or stone [14,57]. In addition, the rabbits are herbivores, and their urine has a high concentration of urate, therefore the anti-calcification activity of PC-SIS was not sufficient to function as expected in the complex *in vivo* environment in rabbits. Whether the PC-SIS material could reduce the formation of bladder stones *in vivo* remained to be further studied in omnivores animal. Nevertheless, current results of ultrasonic examination and tissue sampling all showed remarkable dissolvement of the stones/encrustations over time (8–12 weeks). The detailed process and underlying mechanism are yet to known. We speculated that regeneration of the completed urothelial layer over the transplanted graft at later phase played a key role in the inhibition of stone formation [58].

As shown by morphological observations, the luminal side of the implant was covered by urothelium in all experimental groups at 4 weeks post-operation. This urothelium may develop from the invading cells of the surrounding native urothelium or urothelial progenitor cells [59,60]. Over time, all experimental groups showed complete urothelium regeneration at 8 and 12 weeks, but as revealed by H&E and IF staining the PC-SIS groups especially the PC-SIS 2 group had an urothelium layer more similar to the sham group at the defect areas than the SIS group. The coordination of blood vessels, nerves and smooth muscles growth during bladder wall regeneration also has a great impact on the restoration of bladder functions. Re-vascularization is generally important for implanted patch to provide sufficient blood supply, and re-neuralization participated in neuromuscular responses. Regeneration of smooth muscle is crucial to maintain the structural and functional integrity of the bladder. With unsatisfactory bladder muscular wall regeneration, shrinkage, perforation and leakage may occur. As revealed by H&E and IF staining, PC-SIS groups have shown better regeneration of blood vessels, nerves and smooth muscles than the SIS group. Especially, the PC-SIS 2 group had larger bundles of smooth muscle. Such muscle bundles may help to store or urinate and to maintain a proper intravesical pressure with an increased amount of urine [61].

Urodynamic evaluations were at the whole-organ level pressure/volume relationships, commonly used for assessing changes in bladder compliance [1]. Bladder compliance was defined as the correlation between changes in bladder volume and detrusor pressure (ΔDV/ΔDP det) with a scale in ml/cm H_2O [62,63]. P_{det} was calculated as the subtraction of vesical pressure (P_{ves}) with the abdominal pressure (P_{abd}): $P_{det} = P_{ves} - P_{abd}$. As revealed by the urodynamic measurements at 12 weeks (Fig. 6B), the intravesical pressure curve of both sham group and PC-SIS groups had a decreased slope, indicating an increase in the compliance of the bladder as changes of filling volume had led to a slower rise in intravesical pressure. By contrast, the SIS group had a sharp increase of intravesical pressure. Indeed, further calculation of bladder compliance confirmed the interpretation. These results were also in consistent with the histological results that the PC-SIS groups had better organized and matured bladder muscular layer improving the compliance of the bladder [64,65].

Current study used a bladder defect model with healthy animals, therefore whether the PC-SIS also apply to situations with different disease backgrounds remained to be explored. Besides, further studies are required for ascertain the risk of malignancy for the regenerated bladder tissues for safety concerns. Most importantly, since changes in material properties in particular the mechanical properties may promote the structural and functional tissue remodeling, more detailed analyses are required to clarify the mechanisms of such PC-SIS material for bladder tissue regeneration therapies in further translational studies.

5. Conclusion

PC-SIS materials prepared by crosslinking SIS with 0.5 mg/ml and 1 mg/ml PC showed good biocompatibility, improved mechanical properties, and anti-calcification activities. In a rabbit full-thickness bladder defect model, cystoplasty with the PC-SIS patches had better bladder functions than that with the SIS patch by promoting smooth muscle regeneration, improving bladder compliance and avoiding progressive renal disease. Especially, the 1 mg/ml PC-SIS had a repair outcome similar to the native bladders histologically and functionally. Such PC-SIS material showed potentials as a bladder patch capable of promoting smooth muscle regeneration and bladder function restoration.

Declaration of competing interest

The authors declare that they have no known competing financial interests.

CRediT authorship contribution statement

Xiu-Zhen Zhang: Formal analysis, Methodology, Writing - original draft. **Yan-Lin Jiang:** Methodology, Formal analysis, Writing - original draft. **Jun-Gen Hu:** Formal analysis, Writing - original draft. **Long-Mei Zhao:** Methodology, Formal analysis. **Qiu-Zhu Chen:** Methodology, Formal analysis. **Yan Liang:** Methodology. **Yi Zhang:** Methodology. **Xiong-Xin Lei:** Methodology. **Rui Wang:** Methodology. **Yi Lei:** Methodology. **Qing-Yi Zhang:** Methodology. **Jesse Li-Ling:** Formal analysis, Writing - original draft. **Hui-Qi Xie:** Conceptualization, Formal analysis, Writing - original draft, Funding acquisition.

Declaration of competing interest

This manuscript has been approved by all coauthors. It has not been published or presented elsewhere in part or in entirety and is not under consideration by another journal. We have read and understood your journal's policies, and we believe that neither the manuscript nor the study violates any of these. There are no conflicts of interest to declare.

Acknowledgements

We thank Ms. Hong Wang from Department of Ultrasonic, West China Hospital, Sichuan University, Mr. Ming-Ze Song from Department of urology, West China Hospital, Sichuan University, and Ms. Si-Si Wu from Research Core Facility, West China Hospital, Sichuan University for the technique supports. We thank Xi-Jing Yang and Xiao-Ting Chen form the Animal Experimental Center of West China Hospital for assistance in animal experiments. This work was supported by the National Key R&D Program of China (No. 2017YFC1104702), Sichuan Science and Technology Program (No. 2019JDRC0020) and 1.3.5 project for disciplines of excellence, West China Hospital, Sichuan University (No. ZYJC18002).

Appendix A. Supplementary data

Supplementary data to this article can be found online at https://doi.org/10.1016/j.bioactmat.2020.11.023.

References

[1] F. Ajallouеian, G. Lemon, J. Hilborn, I.S. Chronakis, M. Fossum, Bladder biomechanics and the use of scaffolds for regenerative medicine in the urinary bladder, Nat. Rev. Urol. 15 (3) (2018) 155–174, https://doi.org/10.1038/nrurol.2018.5.

[2] M.E. Chua, W.A. Farhat, J.M. Ming, K.A. McCammon, Review of clinical experience on biomaterials and tissue engineering of urinary bladder, World J. Urol. 38 (9) (2020) 2081–2093, https://doi.org/10.1007/s00345-019-02833-4.

[3] O. Lam Van Ba, S. Aharony, O. Loutochin, J. Corcos, Bladder tissue engineering: a literature review, Adv. Drug Deliv. Rev. 82–83 (2015) 31–37, https://doi.org/10.1016/j.addr.2014.11.013.

[4] S.M. Biers, S.N. Venn, T.J. Greenwell, The past, present and future of augmentation cystoplasty, BJU Int. 109 (9) (2012) 1280–1293, https://doi.org/10.1111/j.1464-410X.2011.10650.x.

[5] D.A. Husmann, Malignancy after gastrointestinal augmentation in childhood, Ther. Adv. Urol. 1 (1) (2009) 5–11, https://doi.org/10.1177/1756287209104163.

[6] Á. Serrano-Aroca, C.D. Vera-Donoso, V. Moreno-Manzano, Bioeng. Approaches Bladder Regeneration 19 (6) (2018) 1796, https://doi.org/10.3390/ijms19061796.

[7] M. Wang, Y.-Q. Li, J. Cao, M. Gong, Y. Zhang, X. Chen, M.-X. Tian, H.-Q. Xie, Accelerating effects of genipin-crosslinked small intestinal submucosa for defected gastric mucosa repair, J. Mater. Chem. B 5 (34) (2017) 7059–7071, https://doi.org/10.1039/c7tb00517b.

[8] S.L. Voytik-Harbin, A.O. Brightman, M.R. Kraine, B. Waisner, S.F. Badylak, Identification of extractable growth factors from small intestinal, submucosa 67 (4) (1997) 478–491, https://doi.org/10.1002/(sici)1097-4644(19971215)67:4<478::Aid-jcb6>3.0.Co;2-p.

[9] Biocompatibility of Small-Intestinal Submucosa in Urinary Tract as Augmentation Cystoplasty Graft and Injectable Suspension, vol. 8(2), https://doi.org/10.1089/end.1994.8.125, 1994, 125 130.

[10] S.F. Badylak, B. Kropp, T. McPherson, H. Liang, P.W. Snyder, Small intestinal submucosa: a rapidly resorbed bioscaffold for augmentation cystoplasty in a dog model, Tissue Eng. 4 (4) (1998) 379–387, https://doi.org/10.1089/ten.1998.4.379.

[11] A. Ayyildiz, K.T. Akgül, E. Huri, B. NuhoğLu, B. Kiliçoğlu, H. ÜStün, M. Gürdal, C. Germiyanoğlu, Use OF porcine small intestinal submucosa IN bladder augmentation IN rabbit: long-term histological outcome, 78(1-2), https://doi.org/10.1111/j.1445-2197.2007.04361.x, 2008, 82 86.

[12] Y. Wang, L. Liao, Histologic and functional outcomes of small intestine submucosa-regenerated bladder tissue, BMC Urol. 14 (2014) 69, https://doi.org/10.1186/1471-2490-14-69.

[13] Y. Zhang, D. Frimberger, E.Y. Cheng, H.K. Lin, B.P. Kropp, Challenges in a larger bladder replacement with cell-seeded and unseeded small intestinal submucosa grafts in a subtotal cystectomy model, BJU Int. 98 (5) (2006) 1100–1105, https://doi.org/10.1111/j.1464-410X.2006.06447.x.

[14] J.E. Nuininga, H.v. Moerkerk, A. Hanssen, C.A. Hulsbergen, J. Oosterwijk-Wakka, E. Oosterwijk, R.P.E. de Gier, J.A. Schalken, T.H.v. Kuppevelt, W.F.J. Feitz, A rabbit model to tissue engineer the bladder, Biomaterials 25 (9) (2004) 1657–1661, https://doi.org/10.1016/s0142-9612(03)00519-2.

[15] F. Zhang, L. Liao, Tissue engineered cystoplasty augmentation for treatment of neurogenic bladder using small intestinal submucosa: an exploratory study, J. Urol. 192 (2) (2014) 544–550, https://doi.org/10.1016/j.juro.2014.01.116.

[16] F. Zhang, L. Liao, Long-term follow-up of neurogenic bladder patients after bladder augmentation with small intestinal submucosa, World J. Urol. 38 (9) (2020) 2279–2288, https://doi.org/10.1007/s00345-019-03008-x.

[17] Á. Serrano-Aroca, M. Llorens-Gámez, Dynamic mechanical analysis and water vapour sorption of highly porous poly(methyl methacrylate), Polymer 125 (2017) 58–65, https://doi.org/10.1016/j.polymer.2017.07.075.

[18] W. Hu, Z. Wang, Y. Xiao, S. Zhang, J. Wang, Advances in crosslinking strategies of biomedical hydrogels, Biomater. Sci. 7 (3) (2019) 843–855, https://doi.org/10.1039/c8bm01246f.

[19] A.S. Aroca, M.M. Pradas, J.L.G. Ribelles, Effect of crosslinking on porous poly (methyl methacrylate) produced by phase separation, Colloid Polym. Sci. 286 (2) (2007) 209–216, https://doi.org/10.1007/s00396-007-1755-0.

[20] N. Reddy, R. Reddy, Q. Jiang, Crosslinking biopolymers for biomedical applications, Trends Biotechnol. 33 (6) (2015) 362–369, https://doi.org/10.1016/j.tibtech.2015.03.008.

[21] G. Cao, Y. Huang, K. Li, Y. Fan, H. Xie, X. Li, Small intestinal submucosa: superiority, limitations and solutions, and its potential to address bottlenecks in tissue repair, J. Mater. Chem. B 7 (33) (2019) 5038–5055, https://doi.org/10.1039/c9tb00530g.

[22] C.E. Schmidt, J.M. Baier, Acellular vascular tissues: natural biomaterials for tissue repair and tissue engineering, Biomaterials 21 (22) (2000) 2215–2231, https://doi.org/10.1016/S0142-9612(00)00148-4.

[23] W. Zhai, J. Chang, K. Lin, J. Wang, Q. Zhao, X. Sun, Crosslinking of decellularized porcine heart valve matrix by procyanidins, Biomaterials 27 (19) (2006) 3684–3690, https://doi.org/10.1016/j.biomaterials.2006.02.008.

[24] X. Wang, B. Ma, J. Chang, Preparation of decellularized vascular matrix by co-crosslinking of procyanidins and glutaraldehyde, Bio Med. Mater. Eng. 26 (1–2) (2015) 19–30, https://doi.org/10.3233/BME-151548.

[25] X. Wang, W. Zhai, C. Wu, B. Ma, J. Zhang, H. Zhang, Z. Zhu, J. Chang, Procyanidins-crosslinked aortic elastin scaffolds with distinctive anti-calcification and biological properties, Acta Biomater. 16 (2015) 81–93, https://doi.org/10.1016/j.actbio.2015.01.028.

[26] M.-P. Gonthier, J.L. Donovan, O. Texier, C. Felgines, C. Remesy, A. Scalbert, Metabolism of dietary procyanidins in rats, Free Radic. Biol. Med. 35 (8) (2003) 837–844, https://doi.org/10.1016/S0891-5849(03)00394-0.

[27] B. Han, J. Jaurequi, B.W. Tang, M.E. Nimni, Proanthocyanidin: A natural crosslinking reagent for stabilizing collagen matrices 65A (1) (2003) 118–124, https://doi.org/10.1002/jbm.a.10460.

[28] Y. Liu, V. Dusevich, Y. Wang, Proanthocyanidins rapidly stabilize the demineralized dentin layer, J. Dent. Res. 92 (8) (2013) 746–752, https://doi.org/10.1177/0022034513492769.

[29] A. Balalaie, M.B. Rezvani, M. Mohammadi Basir, Dual function of proanthocyanidins as both MMP inhibitor and crosslinker in dentin biomodification: a literature review, Dent. Mater. J. 37 (2) (2018) 173–182, https://doi.org/10.4012/dmj.2017-062.

[30] W. Zhai, H. Zhang, C. Wu, J. Zhang, X. Sun, H. Zhang, Z. Zhu, J. Chang, Crosslinking of saphenous vein ECM by procyanidins for small diameter blood vessel replacement, 102(6), https://doi.org/10.1002/jbm.b.33102, 2014, 1190 1198.

[31] J.C. Luo, W. Chen, X.H. Chen, T.W. Qin, Y.C. Huang, H.Q. Xie, X.Q. Li, Z.Y. Qian, Z. M. Yang, A multi-step method for preparation of porcine small intestinal submucosa (SIS), Biomaterials 32 (3) (2011) 706–713, https://doi.org/10.1016/j.biomaterials.2010.09.017.

[32] T. Liu, L. Shi, Z. Gu, W. Dan, N. Dan, A novel combined polyphenol-aldehyde crosslinking of collagen film-Applications in biomedical materials, Int. J. Biol. Macromol. 101 (2017) 889–895, https://doi.org/10.1016/j.ijbiomac.2017.03.166.

[33] L. Zhou, J. Xia, P. Wang, R. Jia, J. Zheng, X. Yao, Y. Chen, Y. Dai, B. Yang, Autologous smooth muscle progenitor cells enhance regeneration of tissue-engineered bladder, Tissue Eng. 24 (13–14) (2018) 1066–1081, https://doi.org/10.1089/ten.TEA.2017.0376.

[34] T. Kokubo, H. Takadama, How useful is SBF in predicting in vivo bone bioactivity? Biomaterials 27 (15) (2006) 2907–2915, https://doi.org/10.1016/j.biomaterials.2006.01.017.

[35] M.Y. Speer, H.Y. Yang, T. Brabb, E. Leaf, A. Look, W.L. Lin, A. Frutkin, D. Dichek, C.M. Giachelli, Smooth muscle cells give rise to osteochondrogenic precursors and chondrocytes in calcifying arteries, Circ. Res. 104 (6) (2009) 733–741, https://doi.org/10.1161/CIRCRESAHA.108.183053.

[36] X. Hou, C. Shi, W. Chen, B. Chen, W. Jia, Y. Guo, C. Ma, G. Ye, J. Kang, J. Dai, Transplantation of human adipose-derived mesenchymal stem cells on a bladder acellular matrix for bladder regeneration in a canine model, Biomed. Mater. 11 (3) (2016), 031001, https://doi.org/10.1088/1748-6041/11/3/031001.

[37] C.C. Roth, F.G. Mondalek, Y. Kibar, R.A. Ashley, C.H. Bell, J.A. Califano, S. V. Madihally, D. Frimberger, H.K. Lin, B.P. Kropp, Bladder regeneration in a canine model using hyaluronic acid-poly(lactic-co-glycolic-acid) nanoparticle modified porcine small intestinal submucosa, BJU Int. 108 (1) (2011) 148–155, https://doi.org/10.1111/j.1464-410X.2010.09757.x.

[38] P. Caione, R. Boldrini, A. Salerno, S.G. Nappo, Bladder augmentation using acellular collagen biomatrix: a pilot experience in exstrophic patients, Pediatr. Surg. Int. 28 (4) (2012) 421–428, https://doi.org/10.1007/s00383-012-3063-0.

[39] A. Seth, Y.G. Chung, E.S. Gil, D. Tu, D. Franck, D. Di Vizio, R.M. Adam, D. L. Kaplan, C.R. Estrada Jr., J.R. Mauney, The performance of silk scaffolds in a rat model of augmentation cystoplasty, Biomaterials 34 (20) (2013) 4758–4765, https://doi.org/10.1016/j.biomaterials.2013.03.038.

[40] Y. Zhang, H.K. Lin, D. Frimberger, R.B. Epstein, B.P. Kropp, Growth of bone marrow stromal cells on small intestinal submucosa: an alternative cell source for tissue engineered bladder, BJU Int. 96 (7) (2005) 1120–1125, https://doi.org/10.1111/j.1464-410X.2005.05741.x.
[41] C. Alberti, Whyever bladder tissue engineering clinical applications still remain unusual even though many intriguing technological advances have been reached? Geka Chiryo 37 (1) (2016) 6–12, https://doi.org/10.11138/gchir/2016.37.1.006.
[42] P. Caione, N. Capozza, D. Zavaglia, G. Palombaro, R. Boldrini, In vivo bladder regeneration using small intestinal submucosa: experimental study, Pediatr. Surg. Int. 22 (7) (2006) 593–599, https://doi.org/10.1007/s00383-006-1705-9.
[43] S. Wu, Y. Liu, S. Bharadwaj, A. Atala, Y. Zhang, Human urine-derived stem cells seeded in a modified 3D porous small intestinal submucosa scaffold for urethral tissue engineering, Biomaterials 32 (5) (2011) 1317–1326, https://doi.org/10.1016/j.biomaterials.2010.10.006.
[44] M. Gou, Y.-Z. Huang, J.-G. Hu, Y.-L. Jiang, X.-Z. Zhang, N.-C. Su, Y. Lei, H. Zhang, H. Wang, H.-Q. Xie, Epigallocatechin-3-gallate cross-linked small intestinal submucosa for guided bone regeneration, ACS Biomater. Sci. Eng. 5 (10) (2019) 5024–5035, https://doi.org/10.1021/acsbiomaterials.9b00920.
[45] C.S. Ku, M. Sathishkumar, S.P. Mun, Binding affinity of proanthocyanidin from waste Pinus radiata bark onto proline-rich bovine achilles tendon collagen type I, Chemosphere 67 (8) (2007) 1618–1627, https://doi.org/10.1016/j.chemosphere.2006.11.037.
[46] J.D. Hartgerink, E. Beniash, S.I. Stupp, Self-assembly and mineralization of peptide-amphiphile nanofibers, Science 294 (5547) (2001) 1684, https://doi.org/10.1126/science.1063187.
[47] R. Kato, S. Nakamura, K. Katayama, K. Yamashita, Electrical polarization of plasma-spray–hydroxyapatite coatings for improvement of osteoconduction of implants, J. Biomed. Mater. Res. 74A (4) (2005) 652–658, https://doi.org/10.1002/jbm.a.30339.
[48] S.R. Peyton, C.M. Ghajar, C.B. Khatiwala, A.J. Putnam, The emergence of ECM mechanics and cytoskeletal tension as important regulators of cell function, Cell Biochem. Biophys. 47 (2) (2007) 300–320, https://doi.org/10.1007/s12013-007-0004-y.
[49] S.R. Peyton, P.D. Kim, C.M. Ghajar, D. Seliktar, A.J. Putnam, The effects of matrix stiffness and RhoA on the phenotypic plasticity of smooth muscle cells in a 3-D biosynthetic hydrogel system, Biomaterials 29 (17) (2008) 2597–2607, https://doi.org/10.1016/j.biomaterials.2008.02.005.
[50] B.-S. Kim, J. Nikolovski, J. Bonadio, D.J. Mooney, Cyclic mechanical strain regulates the development of engineered smooth muscle tissue, Nat. Biotechnol. 17 (10) (1999) 979–983, https://doi.org/10.1038/13671.
[51] J. Nikolovski, B.S. Kim, D.J. Mooney, Cyclic strain inhibits switching of smooth muscle cells to an osteoblast-like phenotype, Faseb. J. : Off. Publ. Feder. Am. Soc. Exper. Biol. 17 (3) (2003) 455–457, https://doi.org/10.1096/fj.02-0459fje.
[52] J.P. Stegemann, R.M. Nerem, Phenotype modulation in vascular tissue engineering using biochemical and mechanical stimulation, Ann. Biomed. Eng. 31 (4) (2003) 391–402, https://doi.org/10.1114/1.1558031.
[53] E. Vardar, H.M. Larsson, E.M. Engelhardt, K. Pinnagoda, P.S. Briquez, J.A. Hubbell, P. Frey, IGF-1-containing multi-layered collagen-fibrin hybrid scaffolds for bladder tissue engineering, Acta Biomater. 41 (2016) 75–85, https://doi.org/10.1016/j.actbio.2016.06.010.
[54] K. Iijima, Y. Igawa, T. Imamura, T. Moriizumi, T. Nikaido, I. Konishi, O. Nishizawa, Transplantation of preserved human amniotic membrane for bladder augmentation in rats, Tissue Eng. 13 (3) (2007) 513–524, https://doi.org/10.1089/ten.2006.0170.
[55] P. Slusarewicz, K. Zhu, T. Hedman, Kinetic characterization and comparison of various protein crosslinking reagents for matrix modification, J. Mater. Sci. Mater. Med. 21 (4) (2010) 1175–1181, https://doi.org/10.1007/s10856-010-3986-8.
[56] Q. Wang, D.D. Xiao, H. Yan, Y. Zhao, S. Fu, J. Zhou, Z. Wang, Z. Zhou, M. Zhang, M.J. Lu, The morphological regeneration and functional restoration of bladder defects by a novel scaffold and adipose-derived stem cells in a rat augmentation model, Stem Cell Res. Ther. 8 (1) (2017) 149, https://doi.org/10.1186/s13287-017-0597-z.
[57] R.L. Ryall, P.K. Grover, V.R. Marshall, Urate and calcium stones–picking up a drop of mercury with one's fingers? Am. J. Kidney Dis. : Off. J. Natl. Kidney Foundation 17 (4) (1991) 426–430, https://doi.org/10.1016/s0272-6386(12)80636-6.
[58] S.S. Talab, A.-M. Kajbafzadeh, A. Elmi, A. Tourchi, S. Sabetkish, N. Sabetkish, M. Monajemzadeh, Bladder reconstruction using scaffold-less autologous smooth muscle cell sheet engineering: early histological outcomes for autoaugmentation cystoplasty, BJU Int. 114 (6) (2014) 937–945, https://doi.org/10.1111/bju.12685.
[59] H.M. Larsson, F. Gorostidi, J.A. Hubbell, Y. Barrandon, P. Frey, Clonal, self-renewing and differentiating human and porcine urothelial cells, a novel stem cell population, PloS One 9 (2) (2014), e90006, https://doi.org/10.1371/journal.pone.0090006.
[60] F.M. Schäfer, K. Algarrahi, A. Savarino, X. Yang, C. Seager, D. Franck, K. Costa, S. Liu, T. Logvinenko, R. Adam, J.R. Mauney, Mode of surgical injury influences the source of urothelial progenitors during bladder defect repair, Stem Cell Rep. 9 (6) (2017) 2005–2017, https://doi.org/10.1016/j.stemcr.2017.10.025.
[61] C. Shi, W. Chen, B. Chen, T. Shan, W. Jia, X. Hou, L. Li, G. Ye, J. Dai, Bladder regeneration in a canine model using a bladder acellular matrix loaded with a collagen-binding bFGF, Biomater. Sci. 5 (12) (2017) 2427–2436, https://doi.org/10.1039/c7bm00806f.
[62] R.L. Harris, G.W. Cundiff, J.P. Theofrastous, R.C. Bump, Bladder compliance in neurologically intact women, Neurourol. Urodyn. 15 (5) (1996), https://doi.org/10.1002/(sici)1520-6777(1996)15:5<483::Aid-nau5>3.0.Co;2-b, 483-8.
[63] M. Kang, M. Kim, M.S. Choo, J.S. Paick, S.J. Oh, Urodynamic features and significant predictors of bladder outlet obstruction in patients with lower urinary tract symptoms/benign prostatic hyperplasia and small prostate volume, Urology 89 (2016) 96–102, https://doi.org/10.1016/j.urology.2015.11.027.
[64] Y. Wang, S. Zhou, R. Yang, Q. Zou, K. Zhang, Q. Tian, W. Zhao, L. Zong, Q. Fu, Bioengineered bladder patches constructed from multilayered adipose-derived stem cell sheets for bladder regeneration, Acta Biomater. 85 (2019) 131–141, https://doi.org/10.1016/j.actbio.2018.12.016.
[65] F. Zhao, L. Zhou, Z. Xu, L. Xu, Z. Xu, W. Ping, J. Liu, C. Zhou, M. Wang, R. Jia, Hypoxia-preconditioned adipose-derived endothelial progenitor cells promote bladder augmentation, Tissue Eng. 26 (1–2) (2020) 78–92, https://doi.org/10.1089/ten.TEA.2019.0045.